Astron. Astrophys. 321, 343–352 (1997)

ASTRONOMY
AND
ASTROPHYSICS

M/L_B and $[Fe/H]$ of elliptical galaxies and the initial mass function

L. Angeletti and P. Giannone

Istituto Astronomico, Università 'La Sapienza', Via Lancisi 29, I-00161 Roma, Italy

Received 7 May 1996 / Accepted 7 October 1996

Abstract. The observed trend of mass-to-light ratio M/L_B versus elliptical galaxy mass M has been interpreted in various ways by different authors in recent years. We explore in greater detail than previously done the hypothesis that the mentioned trend can be ascribed to a systematic change of the initial mass function (IMF) with M. We use a three-segment power-law IMF with mass exponents x_1, x_2, and x_3 for stellar masses m (in $M_\odot$) in the ranges $0.1 < m < 0.3$, $0.3 < m < 2$, and $2 < m < 100$, respectively. The exponent x_1 is considered as a free parameter in the range $0 \div 3.5$, while x_2 and x_3 are determined using relations M/L_B versus M and $[Fe/H]$ versus M as constraints. We find that $x_2 + 3.4\ x_3 \simeq -0.72 \log M + const.$, irrespectively of whether the bottom IMF exponent x_1 varies from a flat to a very steep behaviour. We single out a number of realistic solutions; for all of them $\mathrm{d}x_3/\mathrm{dlog}M = -0.16 \div -0.35$. On the other hand, solutions with $x_2 = const.$, $x_3 = const.$, and x_1 variable with M are to be excluded, being at variance with the observed $[Fe/H] - M$ relationship. We confirm that a variable single-slope IMF is not a very appealing solution since it requires a minimum stellar mass $m_l \gtrsim 0.24$.

Key words: galaxies: elliptical and lenticular - elliptical galaxies: fundamental plane and metallicity

1. Introduction

As is well known (Dressler et al. 1987 hereafter D87; Djorgovski & Davis 1987), elliptical galaxies are located on the so-called fundamental plane (FP) in the three-dimensional parameter space (σ_o, r_e, SB_e) with σ_o the central velocity dispersion, r_e the effective radius, and SB_e the mean effective surface brightness. The FP was re-examined by Bender et al. (1992 hereafter BBF) with the aid of a new coordinate system. BBF found that the FP defined by ellipticals in the Virgo and Coma clusters is very thin, its thickness is constant and implies a very small variation ($\lesssim 12\%$) of the mass-to-light ratio M/L_B at any given mass M or blue luminosity L_B. Moreover, the tilt of the FP implies that M/L_B increases by a factor of 3 when M is increased by a factor of 400 or, equivalently, L_B by a factor of 130. The metallicity range spanned by ellipticals in the BBF sample can only explain a M/L_B increase by a factor of about 1.4 according to, for instance, synthetic models by Buzzoni (1989 hereafter B89 and 1995) or by Worthey (1994 hereafter W94).

Various conjectures were put forward by several authors (Djorgovski & Santiago 1993; Guzmán et al. 1993; Renzini & Ciotti 1993; Ciotti et al. 1996) in order to reproduce the observed FP tilt; among them: i) a multi-slope initial mass function (IMF) similar to that by Scalo (1986), i.e. $\psi(m) \propto m^{-2.7}$ for $m > 2$, $\psi(m) \propto m^{-2.35}$ for $0.3 < m < 2$, and $\psi(m) \propto m^{-x}$ with a variable (with M or L_B) exponent x for $m_l < m < 0.3$ (with m in $M_\odot$ and e.g. $m_l = 0.1$); ii) a variable (with M or L_B) ratio of the dark-to-bright mass and/or a change in the relative spatial distribution of the two kinds of matter; iii) a radially increasing (with M or L_B) anisotropy in the stellar velocity dispersion; iv) a systematic (with respect to M or L_B) deviation of the light distribution from the $r^{1/4}$-law.

Present-day observations do not allow to make an assessment of the above hypotheses. We try an explanation based on a multi-slope IMF with three mass exponents and on the two constraints represented by $M/L_B - M$ and $[Fe/H] - M$ relations. In order to gain an overall insight at a reasonable computational cost, we use the simple (closed-box) approach of chemical evolution (e.g. see Pagel & Patchett 1975). For each model elliptical we obtain the fractional (by number) distribution of stars with respect to metal abundance (by mass) Z and mean abundance $< Z >$. Luminosities L_B and M/L_B ratios are derived from B89 synthetic models. The model quantities M/L_B and $< Z >$ are compared with M/L_B ratios and the mean metallicities of observed ellipticals with the same M (or L_B). The reliability of simple-model results is verified with our computer code of chemical evolution for more realistic models (Angeletti & Giannone 1990 and 1991).

The paper is organized as follows: in Sect. 2 we deal with the multi-slope IMF and the $(M/L_B) - M$ and $[Fe/H] - M$ relations to be used throughout the paper; the simple-model ap-

Send offprint requests to: L. Angeletti

proach is considered in Sect. 3, and model results are presented in Sect. 4 and discussed in Sect. 5.

2. The IMF, M/L-M and [Fe/H]-M relations

Besides the multi-slope IMF, we take into account two observed relations to constrain our model ellipticals. They are referred to galaxy mass M, since M (and not L_B) is an input parameter for the computer code. In the following, M and L_B are given in solar units.

2.1. The multi-slope IMF

The multi-slope IMF is written as a power-law mass spectrum

$$\psi(m) = C\ K_i\ m^{-x_i} \qquad (i = 1, 2, 3) \tag{1}$$

where stellar mass m is in the range from $m_l = 0.1$ to $m_u = 100$; $K_1 = 0.3^{x_1 - x_2}$ and x_1 refer to the range $m_l < m < 0.3$, $K_2 = 1$ and x_2 to $0.3 < m < 2$, and $K_3 = 2^{x_3 - x_2}$ and x_3 to $2 < m < m_u$. Cases with m_l and m_u different from the reference values 0.1 and 100 will also be considered in Sect. 4. The constant C is determined by the normalization condition $\int_{m_l}^{m_u} m\psi(m)\mathrm{d}m = \int_0^{t^*} \sigma(t)\mathrm{d}t$, where $\sigma(t)$ is the star formation rate (i.e. the mass of stars born per unit time) and t^* is the age when the star formation ceased owing to, e.g., a galactic wind. Of course, for a single-slope IMF one has $x_1 = x_2 = x_3 = x$.

2.2. (M/L_B) versus M

The $(M/L_B) - M$ relation is taken from BBF, who introduced a new orthogonal coordinate system (k_1, k_2, k_3) in the 3-dimensional parameter space (σ_o, r_e, SB_e), with $\log(M/L_B) = 3^{0.5}k_3 + const.$ and $\log M = 2^{0.5}k_1 + const.$ The equation of the FP defined by Virgo ellipticals is $k_3 = 0.15k_1 + 0.36$. Thus, one has $M/L_B \propto M^a \propto L_B^{a/(1-a)}$, where $a = 0.15 \times 1.5^{0.5} \simeq 0.184$. With the same structural constants as in BBF (see the caption to their Fig. 2 and their Appendix A) the final relation becomes

$$\log\frac{M}{L_B} = 0.184\ \log M - 1.184\ \log D + 0.3365 \tag{2}$$

where D is the distance (hereafter in Mpc) to the Virgo cluster. BBF adopted $D = 20.7$ from recession velocities; we prefer $D = 16$, which is the median value of two recent determinations of the distance to Virgo from classical Cepheids (Pierce et al. 1994; Freedman et al. 1994). The measured Cepheid distance is independent of the recession velocities and Hubble constant H_o. Galaxy masses (hereafter in $M_\odot$) in the BBF sample range approximately from $M_1 = 5 \times 10^9$ to $M_2 = 2 \times 10^{12}$; from (2) it follows that the mass-to-light ratio M/L_B increases from 4.96 to 14.93 (i.e. by a factor of 3). The same mass range (M_1, M_2) of model ellipticals will be explored in Sect. 4 with the aim of obtaining the observed range of the M/L_B ratios.

2.3. The mean metallicity $[Fe/H]$ versus M

Our estimates of mean abundances $< Z >$ of ellipticals obeying relation (2), are largely conjectural since we only have at our disposal: i) the central index Mg_2 for a few arcsec nuclear regions; ii) the radial gradient $\mathrm{d}Mg_2/\mathrm{dlog}r$ for radial distances $r \leq r_e$ in a few ellipticals; iii) a (theoretical and/or empirical) calibration of the Mg_2 index versus $[Fe/H]$. For the sake of homogeneity of spectroscopic and photometric data we choose a sample of 18 Virgo ellipticals studied by D87 (see Table 1), which span the same magnitude range as the 22 Virgo ellipticals in the BBF sample. The two samples have 14 ellipticals in common.

The published central values of Mg_2 were obtained using a $16'' \times 16''$ aperture, which is practically equivalent to a circular aperture of radius $9''$. Such a fixed aperture radius intercepts, in each elliptical, a linear radius r_o or $\tilde{r}_o = r_o/r_e$, which can be determined from the photometric data in D87. For ellipticals with $M > 10^{11}$ we adopt mean radial gradient $\mathrm{d}Mg_2/\mathrm{dlog}\tilde{r} = -\delta = -0.059$ (with a ± 0.022 dispersion and $\tilde{r} = r/r_e$), as obtained by Davies et al. (1993 hereafter DSP) for radial distances larger than $3''$ and up to $\tilde{r} = 1$ from 13 ellipticals. The DSP and D87 samples have 4 ellipticals in common. For ellipticals with $M < 10^{11}$ we choose $\mathrm{d}Mg_2/\mathrm{dlog}\tilde{r} = -\delta = -0.029\ \log M + 0.26$ (for $\tilde{r} \lesssim 1$), i.e. an increasing gradient δ with increasing mass, according to results by Carollo et al. (1993, their Fig. 11).

We adopt the calibration of Mg_2 versus $[Fe/H]$ as given in W94 and obtained using synthetic single-burst models with (Salpeter's) $x = 2.35$. W94 gives variations $\Delta Mg_2 \simeq -0.0025$ and 0.012 when passing from $x = 2.35$ to 1.35 and 3.35, respectively, at the solar metallicity and age of 12 Gyr. On the other hand, calibrations for x=1.35, 2.35, and 3.35 were also provided by Buzzoni et al. (1992 hereafter BGM) which we use to provide differential estimates. We assume that the measured index Mg_2 refers to a simple stellar population (SSP), i.e. to coeval and chemically homogeneous stars, in particular with the common age of 15 Gyr (the adopted calibration is obtained by linear interpolation between the 12 Gyr and 17 Gyr W94 sequences). This procedure is questionable when applied to observed ellipticals, because: i) the model relation $Mg_2 - [Fe/H]$ rests on the abundance ratios of local calibrating stars, which appear to be different from those in ellipticals (Worthey et al. 1992 hereafter WFG; W94; DSP; Weiss et al. 1995); ii) ellipticals are not chemically homogeneous systems, as is shown by radial gradients of Mg_2 and other spectral features (WFG; DSP; Carollo et al. 1993). As a consequence, the measured Mg_2 and inferred $[Fe/H]$ are in fact related to a mix of SSPs seen along the line-of-sight. Since synthetic models of composite stellar populations are not avalaible, we assume (as e.g. in DSP) that the mean metallicity of SSPs, involved in the measured Mg_2, is reasonably close to that derived from single-burst models.

In the W94 calibration a mean slope $\mathrm{d}Mg_2/\mathrm{d}[Fe/H] = \gamma \simeq 0.183$ is a good approximation to the γ values in the range $0.18 \lesssim Mg_2 \lesssim 0.36$. From the BGM calibration γ turns out to be fairly constant and approximately equal to 0.133 (for x=1.35,

Table 1. Metallicities $[Fe/H]_o$ (within an aperture radius $\tilde{r}_o$), $[Fe/H]_e$ (at r_e), and $[Fe/H]$ (global average) for the Virgo ellipticals in the D87 sample, from the W94 calibration and for an age of 15 Gyr (see text)

Name	B_T	$\tilde{r}_o$	Mg_2	$\log\frac{M}{M_\odot}$	$[Fe/H]_o$	$[Fe/H]_e$	$[Fe/H]$
N4365	10.63	0.153	0.311	11.361	0.208	-0.113	-0.073
N4374	10.15	0.169	0.310	11.597	0.202	-0.109	-0.069
N4387	12.86	0.572	0.236	10.268	-0.202	-0.364	-0.336
N4406	9.88	0.095	0.299	11.729	0.142	-0.219	-0.179
N4434	12.80	0.465	0.241	10.298	-0.175	-0.350	-0.321
N4458	12.73	0.314	0.212	10.332	-0.334	-0.545	-0.517
N4464	13.62	1.727	0.227	9.896	-0.252	-0.317	-0.302
N4472	9.51	0.106	0.335	11.910	0.339	-0.214	-0.123
N4473	11.19	0.344	0.304	11.087	0.170	-0.074	-0.034
N4478	12.16	0.627	0.253	10.611	-0.109	-0.309	-0.266
N4486	9.57	0.091	0.324	11.881	0.279	-0.087	-0.047
N4551	12.70	0.487	0.241	10.347	-0.175	-0.354	-0.323
N4552	10.87	0.314	0.320	11.244	0.257	0.004	0.044
N4564	11.92	0.378	0.278	10.729	0.027	-0.231	-0.183
N4621	10.70	0.208	0.312	11.327	0.213	-0.077	-0.037
N4636	10.22	0.091	0.316	11.562	0.235	-0.130	-0.090
N4649	9.73	0.117	0.359	11.802	0.471	-0.069	0.021
N4660	12.19	0.703	0.270	10.597	-0.016	-0.203	-0.162

2.35, 3.35) in the range $0.10 \lesssim Mg_2 \lesssim 0.36$ (Fig. 1). From the central values of Mg_2, the adopted mean slope δ, and an $\tilde{r}^{1/4}$-law it follows that γ is roughly constant in a central circular region containing, in projection, from 50% to about 75% of the masses of the galaxies in the D87 sample.

We make the simplifying assumption that the above values of both δ (which is not observationally known for $r > r_e$) and γ also apply beyond r_e in the ellipticals of the D87 sample. Thus, we can write $\mathrm{d}[Fe/H] = -(\delta/\gamma)\mathrm{dlog}\tilde{r}$ or, with a solar relative element abundance distribution, $Z(\tilde{r}) = Z_e\tilde{r}^{-\epsilon}$, where $\epsilon = \delta/\gamma$ and $Z_e = Z(1)$. Under the assumption that the local mass-to-light ratio is independent of $\tilde{r}$, we compute an average Z_o of $Z(\tilde{r})$ within $\tilde{r}_o$ by weighting $Z(\tilde{r})$ with the $\tilde{r}^{1/4}$-law, then we compare Z_o with the abundance inferred from the observed central (i.e. within $\tilde{r}_o$) Mg_2, and thus obtain Z_e. Finally, the mean abundance follows as (Young 1976)

$$< Z >= Z_e \, \frac{\beta^{4\epsilon}}{\Gamma(8)} \, \Gamma(8 - 4\epsilon) \qquad (3)$$

where β = 7.66925, Γ is the Eulerian gamma function, and ϵ corresponds to the region within r_e.

Some trial computions are made with δ behaving as the local escape velocity (Franx & Illingworth 1990; DSP), or with a variable γ (according to the W94 calibration), for several ellipticals in the D87 sample. Mean abundances $< Z >$ turn out to be lower by about 25%, on the average, than those computed with Eq. (3).

Table 1 gives the results for the D87 sample using Eq. (3) and the W94 calibration with γ from the central Mg_2. Data in columns 1 to 4 are from D87 and give NGC number, total blue (apparent) magnitude B_T, aperture radius $\tilde{r}_o$, and central Mg_2, respectively. The mass M, from Eq. (2) with D = 16, is in column 5, the index $[Fe/H]_o = \log(Z_o/Z_\odot)$ (with $Z_\odot$ = 0.0169), corresponding to the central Mg_2, is in column 6, while $[Fe/H]_e = \log(Z_e/Z_\odot)$ and $[Fe/H] = \log(< Z > /Z_\odot)$ are in columns 7 and 8, respectively.

The central (index zero) and mean values of $[Fe/H]$ in Table 1 are also shown in the top panel of Fig. 2 together with the regression lines $[Fe/H]_o = -0.163\ B_T + 1.912$ and $[Fe/H] = -0.087\ B_T + 0.815$. $[Fe/H]_o$ and $[Fe/H]$ for the D87 galaxies are also computed with the BGM calibration. The results are shown in the bottom panel of Fig. 2 together with regression lines (for x = 2.35) $[Fe/H]_o = -0.215\ B_T + 2.482$ and $[Fe/H] = -0.105\ B_T + 0.895$. The mean metallicities $[Fe/H]$ from BGM are smaller, by up to $\Delta[Fe/H]$ = 0.17, than those from W94; the discrepancy is mainly due to the different slopes γ (see WFG). The regression lines $[Fe/H] = -0.106\ B_T + 0.978$ (for x=1.35) and $[Fe/H] = -0.101\ B_T + 0.699$ (for x = 3.35) are also shown in the bottom panel of Fig. 2.

Each $[Fe/H] - B_T$ relation combined with Eq. (2) leads to an $[Fe/H] - M$ relation depending on the IMF mass exponent x. One obtains (with $M_{B,\odot}$ = 5.51 mag and zero dust absorption, see DSP)

$$[Fe/H] = q(x)\ \log\frac{M}{D} + g(x) \qquad (4)$$

where $q(x)$ and $g(x)$ account for the dependence on x. The functions $q(x)$ and $g(x)$ are estimated according to the differential (with respect to x) behaviours of the $Mg_2 - [Fe/H]$ and $[Fe/H] - B_T$ relations from BGM and are adjusted to fit ΔMg_2 as given in W94 for different x at $[Fe/H]$=0. In practice, $q(x) \simeq q$ = 0.1772 and $g(x)$ is an interpolating function

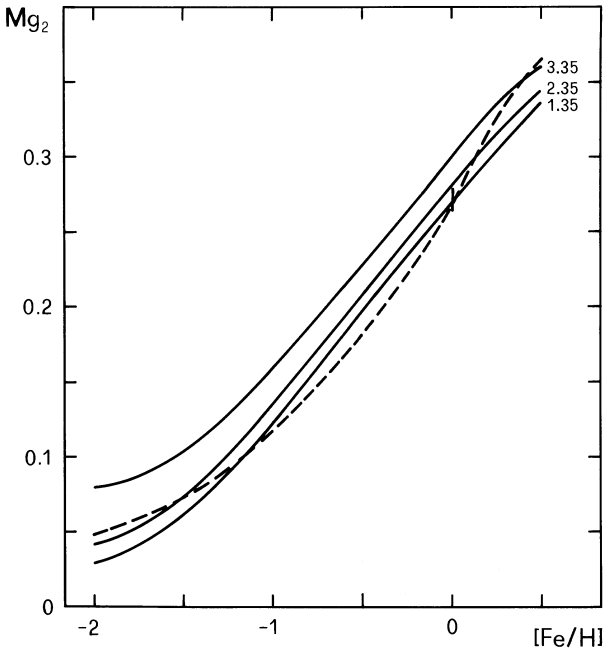

Fig. 1. The $Mg_2 - [Fe/H]$ relation as calibrated according to BGM (solid lines are labeled with IMF mass exponents) and W94 (the dashed line is for Salpeter's mass exponent, the vertical tick is for mass exponents from 1.35 to 3.35). Both calibrations are for a 15 Gyr single-burst population

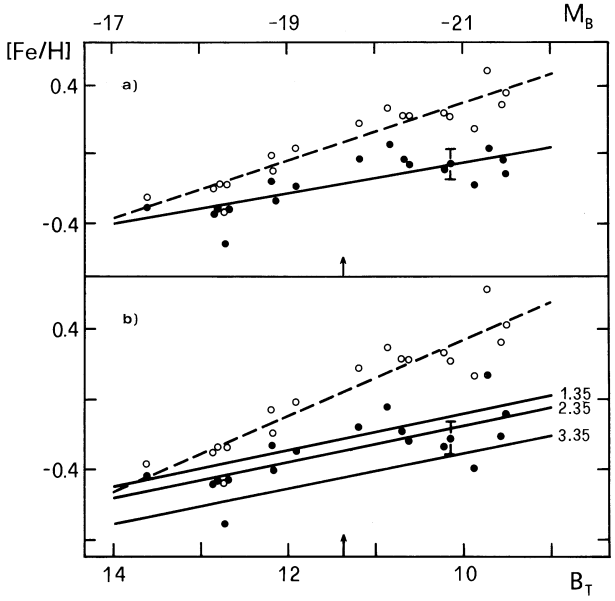

Fig. 2. a The mean index $[Fe/H]$ (filled circles) and central index $[Fe/H]_o$ (open circles) against total apparent blue magnitude B_T for the Virgo ellipticals in the D87 sample. Metallicities are from the $Mg_2 - [Fe/H]$ relation, as calibrated according to W94 for Salpeter's mass exponent and an age of 15 Gyr. The regression lines $[Fe/H] - B_T$ (solid line) and $[Fe/H]_o - B_T$ (dashed line) are also shown. The absolute magnitude M_B (for D=16 Mpc) is given on the upper scale. The scatter, due to the spread ± 0.022 in the observed radial gradients $\mathrm{d}Mg_2/\mathrm{dlog}\tilde{r}$, is shown for a giant elliptical. The vertical arrow marks the location of an elliptical with $M = 10^{11} M_\odot$; **b** As in the above panel, but for the $Mg_2 - [Fe/H]$ relation as calibrated according to BGM. IMF mass exponents label the curves

between -1.892, -1.908, and -1.967 for x = 1.35, 2.35, and 3.35, in that order. Eq. (4) with D = 16 and x = 2.35 indicates that ellipticals in the mass range (M_1, M_2) span the metallicity range $-0.403 \leq [Fe/H] \leq 0.058$. From BGM one obtains that q=0.2142 and $g(x)$ be interpolated between -2.330, -2.397, and -2.564 for x = 1.35, 2.35, and 3.35, respectively.

2.4. Uncertainties in metal abundance

As mentioned above, Eq. (4) probably overestimates true metal abundances by about 25%, owing to our poor knowledge of radial gradient $\mathrm{d}Mg_2/\mathrm{dlog}r$. In addition, Eq. (4) is affected by uncertainties arising from discrepancies between existing $Mg_2 - [Fe/H]$ calibrations (for a synoptic view see for instance Fig. 1 in WFG), which are due to differences in the underlying star evolution models and spectral calibrations adopted by different authors (Charlot et al. 1996; Weiss et al. 1995). With reference to the D87 sample, the above-mentioned discrepancies give rise to an uncertainty of up to $\Delta[Fe/H] \simeq \pm 0.2$. Such an uncertainty will be taken into account in Sect. 4.3 by a boundary variation of our adopted metallicity range.

A further uncertainty is due to our lack of a $Mg_2 - [Fe/H]$ relation for composite star systems. To compensate partly for this defect, in Sect. 4.4 we shall use luminosity-weighted metallicities and compare them with observed metallicities from Eq. (4). Finally, the synthetic spectral index Mg_2 was computed recently by Weiss et al. (1995) for Mg/Fe ratios larger than the solar ratio and, in particular, with the Mg-mass fraction of Z larger than the solar value (which more directly matters in our paper). From the very few cases as yet published, the ensuing uncertainties appear well included in the ones discussed so far. Obviously, if non-solar ratios are considered, the metallicity notation $[Fe/H]$ has to be replaced by $\log < Z > /Z_\odot$.

3. Simple-model approach

We recall that in the simple (closed-box) model of chemical evolution (e.g. see Pagel & Patchett 1975; Pagel 1989) the fractional (by number) distribution $\mathrm{d}N/N_t$ of stars with respect to abundance Z is given by

$$\frac{\mathrm{d}N}{N_t} \propto \frac{1}{p} \exp(-\frac{Z}{p})\, \mathrm{d}Z \tag{5}$$

where p is the metal yield and N_t the total number of stars. The metal yield is evaluated as

$$p = \frac{\int_{m'}^{100} m_Z(m)\psi(m)\mathrm{d}m}{\int_{m_l}^{m'} m\psi(m)\mathrm{d}m + \int_{m'}^{100} m_R(m)\psi(m)\mathrm{d}m} \tag{6}$$

where $m_Z(m)$ is the 'stellar yield', i.e. the mass of new metals ejected into the interstellar medium by a star of mass m, $m_R(m)$ is the remnant mass of a star with initial mass m, and

the denominator is the mass 'locked up' in remnants (for m' see below). Assuming a solar relative element abundance distribution and neglecting the contribution from intermediate mass stars ($m < 8$), we evaluate $m_Z(m)$ using the magnesium yields by Woosley (1987). To a very good approximation, it is

$$\int_8^{100} m_Z(m)\psi(m)\mathrm{d}m \simeq 2334\ CK_3 \times \exp(-4.6378\ x_3 + 0.1997\ x_3^2)$$

We also adopt $m_R(m)$=1.4 for $m \geq 8$ and $m_R(m) = 0.077\ m +$ 0.48 for $m < 8$ (Renzini & Ciotti 1993).

In the case of the assumption of instantaneous gas recycling, the stellar mass m' is related to the presumed time duration of the star formation. We take $m' = 3$; note that p (with e.g. Salpeter's single-slope IMF) increases by only 25% when m' is decreased from 8 to 1 and a spread of ± 1 around m'=3 implies a negligible $\pm$4% dispersion of p . However, stellar lifetimes τ_m show a much larger variation; one has τ_4 = 0.194 Gyr, τ_3 = 0.44 Gyr, and τ_2 = 1.4 Gyr according to Schaller et al. (1992).

Finally, the mean abundance $< Z >$ is given as

$$< Z >= p\ (1 + \frac{f_w}{1 - f_w}\ \ln f_w) \qquad (7)$$

where f_w is the fractional gas mass which was left when star formation stopped and was eventually removed by a galactic wind. We derive $< Z >= p$ from Eq. (7) in the limit f_w=0 (complete gas exhaustion) according to the findings by Rich (1992) for the galactic bulge.

It is well known (e.g. Pagel and Patchett 1975) that the results from the simple model are independent of any assumed value of the star-formation rate $\sigma(t)$. However, in order to better clarify the present approach, we write $\sigma(t) = \nu M_g(t)$ where ν^{-1} is the time-scale of the star formation and $M_g(t)$ the gas mass at time t. The simple model predicts $M_g(t) = M_i f(t)$ and $\int_0^{t^*} \sigma(t)\ \mathrm{d}t = M_i[1 - f(t^*)]/\alpha$, $\sigma(t)$ being the star-formation rate, t^* the age when the star formation ceased owing to, e.g., a galactic wind, M_i the initial gas mass, and $f(t)$=exp($-\nu\alpha t$); α is the ratio of the mass locked up to $\int_0^{t^*} \sigma(t)\ \mathrm{d}t$. The limit $f_w = 0$ is safely reached when $f(t)$ decreases to, for instance, $f_w = f(t^*) = 0.001$ (implying $< Z >= 0.993\ p$). The parameter $\nu = -\ln f_w/(\alpha t^*)$ can be evaluated, to an order of magnitude, by adopting f_w= 0.001, a mean value α=0.8 (α ranges from $\simeq 0.75$ to $\simeq 0.95$ in the computations in Sect. 4), and $t^* \gtrsim \tau_3$. One obtains $\nu^{-1} \gtrsim 0.05$ Gyr and a mass locked up $M_i[1 - f(t^*)] = 0.999\ M_i$ at age t^*. The mass shed by evolved stars after an age t^* is assumed to have been removed by a galactic wind.

M/L_B ratios and L_B luminosities are obtained by interpolation between synthetic single-burst models in B89, which are given for five metallicities ($Z = 10^{-4},\ 10^{-3},\ 10^{-2},\ 0.017$, and 0.03) and three single-slope IMF exponents (x = 1.35, 2.35, and 3.35), and m_l=0.1. In addition to the B89 models we also use those for Z = 0.1 by Buzzoni (1995). Mild extrapolations for x below 1.35 and above 3.35, and for Z below 10^{-4} and above 0.1, are made, when necessary. We choose B89 models with red-horizontal-branch morphology, a mass-loss parameter η = 0.3, and age of 15 Gyr. M/L_B ratios in B89 only refer to bright stars. We include remnant masses from stars with $m > m_{RGT}$ (initial mass of stars at the red-giant tip). At 15 Gyr $m_{RGT} \lesssim 1.2$ for $[Fe/H] \lesssim 0.8$ (VandenBerg & Laskarides 1987). We approximate m_{RGT} with the turn-off mass m_{TO} as tabulated in B89. Star masses in the ranges corresponding to the exponents x_1 and x_2 correspond to bright star models in B89. When $x_1 \neq x_2$, the M/L_B ratios from B89 are modified according to the assumption that the contribution of the low-mass stars (i.e. $m < 0.3$) to L_B can be neglected. From Copeland et al. (1970, their Table 5) and with the same procedure as described in Renzini & Buzzoni (1986), we estimate that low-mass stars contribute 2% or 3% to the main-sequence (with m_{TO}=0.9) luminosity in the B band for x_2=3.5 and x_2=4, respectively. Therefore, our results are fairly correct as long as the relative contribution of the low-mass stars to L_B is smaller than (or at least equal to) our estimate. According to this latter assumption, in the following we shall use x_2 instead of x in Eq. (4) when adopting a multi-slope IMF for 15 Gyr old ellipticals.

4. Model results

For any given mass M one obtains M/L_B from Eq. (2). However, x needs to be specified, besides M, to obtain $[Fe/H]$ from Eq. (4). The exponent x is unknown at the beginning, therefore one should resort to an iterative procedure starting with an initial guess, e.g. Salpeter's 2.35. Then, the simple model approach would give a new value of x, which could be used to obtain a new $[Fe/H]$, and so on until convergence would be achieved. However, when x is changed from 3.35 to 1.35, $[Fe/H]$ changes by only 0.075, according to the adopted W94 calibration. Therefore, in a first approximation, the iterative procedure can be avoided and $[Fe/H]$ will be derived from (4) with a fixed x = 2.35. Nevertheless, some cases with multi-slope IMF will be dealt with the iterative procedure to show the (small) discrepancy of simple-model results with respect to the exact ones.

Combining Eq. s (2) and (4) we obtain

$$\log\frac{M}{L_B} = 0.184\ \frac{[Fe/H] - g(x)}{q} - \log D + 0.3365 \qquad (8)$$

with $x = x_2$ for a multi-slope IMF, as mentioned at the end of the above section. When the galaxy mass M is in the range 5×10^9 to 2×10^{12}, M/L_B increases from 4.96 to 14.93, and $[Fe/H]$ from -0.403 to 0.058 (for D=16 and x = 2.35). The metallicity range would change from $[Fe/H] = -0.577$ to -0.020 according to the BGM calibration.

4.1. Single-slope IMF

We first investigate the case of a single-slope IMF with x and m_l as free parameters. Two sets of curves, obtained with variable m_l (or x) at constant x (or m_l), are shown in Fig. 3. They are almost

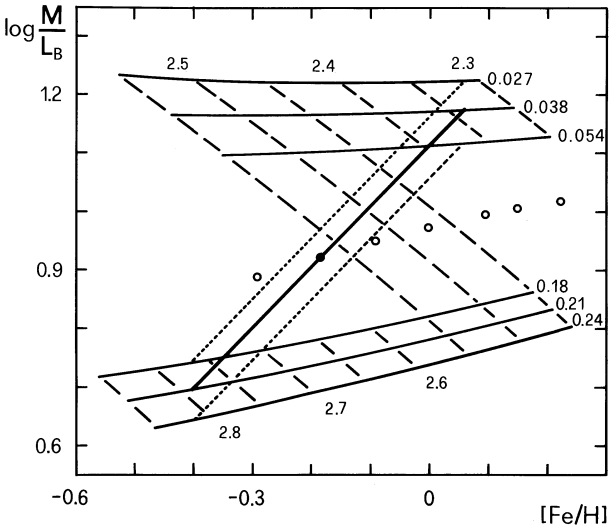

Fig. 3. Single-slope IMFs: thin solid curves correspond to models with constant m_l values (the curves are labeled), thin dashed curves to models with constant IMF mass exponents x (the curves are labeled). Circles refer to models with x=2.35, m_l=0.1, and f_w= 0, 0.05, 0.1, 0.2, 0.3, 0.4, and 0.5 (from right to left). The observational $M/L_B - [Fe/H]$ relation is shown (thick solid line) together with the spread of $\pm 12\%$ in the observed M/L_B ratios (dotted lines)

perpendicular to the observational relation (8) with $x = 2.35$. Therefore, to fit observations both parameters x and m_l must be varied simultaneously. From interpolation we find solutions

$$x = -0.983\ [Fe/H] + 2.394 = -0.946 \log\frac{M}{L_B} + 3.448$$
$$m_l = -0.367\ [Fe/H] + 0.059 = -0.353 \log\frac{M}{L_B} + 0.453 \quad (9)$$

with $2.34 < x < 2.79$ and $0.038 < m_l < 0.207$. Eq. s (9) give $x = 2.68\ m_l + 2.235$. From (9) and Fig. 3 we infer that the observed spread affecting relation (8) can be accounted for by an average spread $\Delta x \simeq \pm 0.02$ or $\Delta m_l \simeq \pm 0.02$. However, the lower end of relation (8) can only be reproduced at the cost of removing the low-mass stars ($m \lesssim 0.24$). This latter circumstance makes the single-slope hypothesis not very attractive (Renzini & Ciotti 1993).

Fig. 3 also shows a set of models with fixed x (= 2.35) and m_l (= 0.1), and no complete gas exhaustion, i.e. abundances $< Z >$ are from Eq. (7) with $0 < f_w \leq 0.5$, where the upper value of f_w is dictated by stability considerations (e.g. see Hills 1980; Mathieu 1983). The above range of f_w gives a 0.5 spread in $[Fe/H]$, but M/L_B varies by a small factor of 1.35 (half of the requested value). Therefore, the galactic wind hypothesis alone could reproduce the observed metallicity range, but cannot fully explain the range of observed M/L_B ratios. The failure of the galactic wind approach to reproduce the observed M/L_B ratios in ellipticals was also noticed recently by Bressan et al. (1994) and earlier by Arimoto and Yoshii (1987).

4.2. Multi-slope IMF

In the case of a multi-slope IMF there is no unique solution, since we have four free parameters (x_1, x_2, x_3, m_l) and only relations (2) and (4) as constraints. In order to simplify matters, we adopt $m_l = 0.1$ as a standard value and consider x_2 and x_3 as functions of x_1 in the range $x_1 = 0 \div 3.5$. We search for solutions $x_2(x_1)$ and $x_3(x_1)$ satisfying the adopted constraints for galaxy masses M_1, $M' = 10^{11}$, and M_2. They are plotted in Fig. 4 and listed in the first three rows of Table 2 for $x_1 = 0,\ 1,\ 2$, and 3 (columns 4 to 11), together with M/L_B (column 2) and $[Fe/H]$ (column 3).

One obtains (to a fairly good approximation) from B89 models

$$\log L_B = -0.310\ [Fe/H] + 0.100\ x_2 + \log C - 0.569$$

in the range $1.35 \leq x_2 \leq 3.35$ and for $-0.5 \leq [Fe/H] \leq 0.5$, where L_B is the total luminosity obtained with the weighting function (5). An acceptable approximation for the M/L_B values in Table 2 can be achieved from L_B^{-1} multiplied by the mass locked up [the denominator in (6) with $m' = m_{TO}$] at the age of 15 Gyr and evaluated with $m_{TO} \simeq 0.9$.

Numerical interpolation between the first three rows of Table 2 leads to (hereafter $y = \log M/M'$):

$$x_2 \simeq 0.437\ y - 0.050\ y^2 - 0.217\ x_1 - 0.064\ x_1^2 + 3.413$$
$$x_3 \simeq -0.349\ y\ + 0.025\ y^2 + 0.063\ x_1 + 0.020\ x_1^2 + 2.305 \quad (10)$$

or, to a first order approximation,

$$x_2 + 3\ x_3 \simeq -0.610\ y\ +\ 10.328$$
$$x_2 + 1.25\ x_3 + (0.197\ x_1 + 0.350)^2 \simeq 6.417 \quad (11)$$

with $0 \leq x_1 \lesssim 3.5$ and $-1.3 \leq y \leq 1.3$. Moreover, from (11) one has $\mathrm{d}x_2/\mathrm{dlog}M \simeq -3\ \mathrm{d}x_3/\mathrm{dlog}M - 0.610$, a relation which will be useful in the following.

Eqs. (2) and (4) can be satisfied by multi-slope IMFs ranging from a flat ($x_1 = 0$) to a steep ($x_1 \simeq 3.5$) behaviour for low-mass stars ($m < 0.3$). All the solutions can be drawn from (10). Solutions with $x_2 = const.$ only exist in the narrow range $2.47 \lesssim x_2 \lesssim 2.76$ and can be found in the horizontal strip shown in Fig. 4. Indeed, lines parallel to the x_1 axis intersect the curves $x_2(x_1)$, for $M_1 \leq M \leq M_2$, only if they are located in the strip. The corresponding x_3 values can be read for each value of M from the x_1 values of the above intersections in the same Fig. 4.

Analogously, solutions with $x_2 = x_1$ (for $2.00 \lesssim x_1 \lesssim 2.82$) or with $x_3 = x_1$ (for $2.08 \lesssim x_1 \lesssim 3.30$) can be obtained in Fig. 4 from the intersections of the diagonal line with curves $x_2(x_1)$ or $x_3(x_1)$, respectively. Solutions with $x_2 = x_3$ can be found by interpolation in Fig. 4, according to (10); they exist for $0 \leq x_1 \lesssim 3.5$ and $2.78 \lesssim x_2 = x_3 \lesssim 3.60$. Solutions with

Table 2. Multi-slope IMF: mass exponents $x_2(x_1)$ and $x_3(x_1)$, obeying Eq. s (2) and (4), for three galaxy masses. The first three rows are from the simple model, the fourth row from a more realistic model (see text)

$M/M_\odot$	M/L_B	$[Fe/H]$	$x_1 = 0$		$x_1 = 1$		$x_1 = 2$		$x_1 = 3$	
			x_2	x_3	x_2	x_3	x_2	x_3	x_2	x_3
5×10^9	4.96	-0.403	2.76	2.80	2.42	2.91	2.01	3.03	1.39	3.21
1×10^{11}	8.60	-0.172	3.41	2.30	3.13	2.39	2.72	2.51	2.17	2.68
2×10^{12}	14.93	0.058	3.90	1.89	3.63	1.97	3.25	2.07	2.72	2.22
"	"	"	3.83	1.97	3.52	2.07	3.05	2.23	2.21	2.55

Table 3. Multi-slope IMF: mass exponents $x_2(x_1)$ and $x_3(x_1)$ for different metallicities $[Fe/H]$ at constant M/L_B

M/L_B	$[Fe/H]$	$x_1 = 0$		$x_1 = 1$		$x_1 = 2$		$x_1 = 3$	
		x_2	x_3	x_2	x_3	x_2	x_3	x_2	x_3
4.96	-0.700	3.13	2.86	2.82	2.97	2.34	3.14	1.80	3.31
"	-0.500	2.90	2.81	2.57	2.92	2.14	3.06	1.56	3.23
"	-0.300	2.59	2.79	2.26	2.89	1.85	3.01	1.11	3.21
10.00	-0.403	3.89	2.23	3.61	2.32	3.21	2.44	2.65	2.62
"	0.058	3.34	2.17	3.06	2.25	2.67	2.36	2.13	2.51
14.93	-0.100	4.08	1.91	3.81	1.99	3.42	2.10	2.90	2.25
"	0.200	3.73	1.87	3.46	1.95	3.08	2.05	2.56	2.20

$x_3 = const.$ only exist in a subset (M_a, M_b), with $M_b \simeq 20\ M_a$ and $M_1 \leq M_a < M_b \leq M_2$. Finally, Eq. s (10) show that $x_1 = x_2 = x_3$ ($\simeq 2.53$) only occurs around $M = 1.5 \times 10^{11}$. A few solutions are plotted in Fig. 5 as functions of galaxy mass M.

Summing up, constraints (2) and (4) can be met by different sets (x_1, x_2, x_3) according to (10). Some of them are:

1. $x_1 = const.$, with $0 \leq x_1 \lesssim 3.5$,
2. $x_2 = const.$, with $2.47 \lesssim x_2 \lesssim 2.76$,
3. $x_3 = const.$, only in subset (M_a, M_b) with $M_b \simeq 20 M_a$ and $M_1 \leq M_a < M_b \leq M_2$,
4. $x_2 = x_1$ in the range $2.00 \lesssim x_1 = x_2 \lesssim 2.82$,
5. $x_3 = x_1$ in the range $2.08 \lesssim x_1 = x_3 \lesssim 3.30$,
6. $x_2 = x_3$ in the range $2.36 \lesssim x_2 = x_3 \lesssim 2.78$
7. $x_1 = x_2 = x_3 \simeq 2.53$ for $M \simeq 1.5 \times 10^{11}$.

Solutions 1), 2), 4), 5), and 6) hold in the whole range (M_1, M_2), while solution 3) exists in a subset of the reference range (M_1, M_2), and solution 7) only around $M = 1.5 \times 10^{11}$. Apart from 3) and 7), all the remaining solutions give a quasi-linear $x_3 - \log M$ relation with $\mathrm{d}x_3/\mathrm{dlog}M = -s$, where $s = 0.16 \div 0.35$ (e.g. see Fig. 5). Consequently, $\mathrm{d}x_2/\mathrm{dlog}M \simeq 3s - 0.61$ is positive (or negative) when $s > 0.20$ (or < 0.20). It should also be noted that solutions with a variable x_1 and constant x_2 and x_3 are not allowed by (10), that is, a Scalo (1986) multi-slope IMF with x_1 as a free parameter is not viable for ellipticals. Moreover, models with $x_1 < 0$ or > 3.5 would require x_2 values larger than 4 or close to zero (i.e. well above 3.35 or below 1.35) and a very uncertain evaluation of the contribution of low-mass stars to L_B. Therefore, they cannot be extrapolated safely from B89.

4.3. Simple-model tests

In order to test the reliability of the simple model we made some trial computations with our computer code of chemical evolution (Angeletti & Giannone 1990, 1991, and 1997) with: i) magnesium yields from Woosley (1987); ii) stellar lifetimes τ_m from Schaller et al. (1992); iii) M/L_B ratios from B89 or W94 (they are in a good agreement, see W94). Constraints (2) and (4) require $\nu^{-1} \simeq 0.03$ Gyr, i.e. a value close to the free-fall time for M_1, and the (protogalaxy) fragment-collision time for M_2. The fourth row in Table 2 gives, for instance, the case for M_2. By comparing the two bottom rows in Table 2 we find that the simple model retains the qualitative behaviour of solutions from more realistic models.

We now investigate the dependence of the results in Sect. 4.2 on metallicity for the BBF sample, as mentioned in Sect. 2.4, and on M/L_B. We consider masses M_1 and M_2 and search for solutions at constant M/L_B and variable metallicity, and viceversa. The results are listed in Table 3, which is arranged as Table 2. They indicate that x_3, for whatever fixed x_1, is practically controlled by the M/L_B ratio alone, being marginally affected by the adopted $[Fe/H]$; whereas x_2 depends equally on M/L_B and $[Fe/H]$ and may have the same value for different mass-to-light ratios and metallicities.

We also estimate the variations $(\Delta x_2, \Delta x_3)$ of the mass exponents x_2 and x_3 (at constant x_1) that are brought about by a dispersion of $\pm 12\%$ in the M/L_B ratios at constant $[Fe/H]$ or by

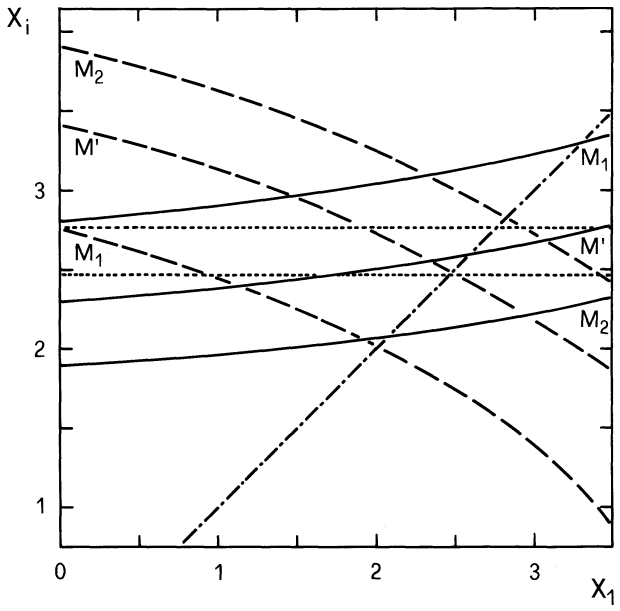

Fig. 4. Mass exponents x_i (i=2, 3) of multi-slope IMFs as functions of x_1 for models with various masses labeling the curves; dashed curves refer to x_2, solid curves to x_3. The horizontal strip bounded by dotted lines corresponds to the region where solutions with $x_2 = const.$ can be found. The diagonal dotted-dashed line identifies solutions with $x_2 = x_1$ or $x_3 = x_1$ (see text)

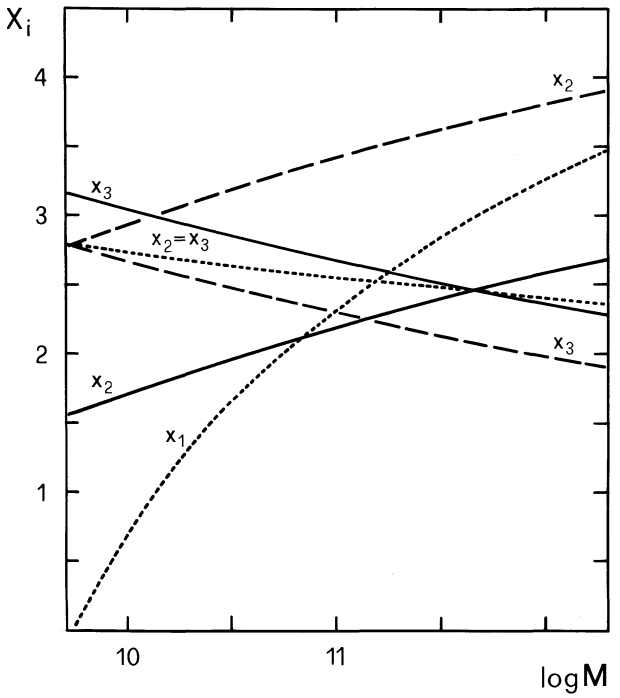

Fig. 5. Some solutions for mass exponents x_i (i=1, 2, 3) of multi-slope IMFs as functions of galaxy mass M (in $M_\odot$). Dashed and solid curves refer to x_2 and x_3 (which give label for the curves) corresponding to solutions with $x_1 = 0$ and $x_1 = 3$, respectively. Dotted curves labeled by x_1, x_2, and x_3 give the particular solution with $x_2 = x_3$

Table 4. Variations of x_2 and x_3 induced by a $\pm 12\%$ dispersion of the M/L_B ratios or a ± 0.1 scatter of metallicities $[Fe/H]$ for galaxy mass M' and listed values of x_1 (for each x_1 the first row corresponds to increasing M/L_B and $[Fe/H]$)

x_1	$\Delta(M/L_B)$		$\Delta[Fe/H]$	
	Δx_2	Δx_3	Δx_2	Δx_3
0	0.17	-0.08	-0.13	-0.01
	-0.20	0.10	0.12	0.01
1	0.17	-0.08	-0.13	-0.01
	-0.21	0.10	0.12	0.02
2	0.18	-0.09	-0.13	-0.01
	-0.22	0.11	0.12	0.02
3	0.17	-0.08	-0.12	-0.03
	-0.20	0.09	0.11	0.03

a scatter of ± 0.1 in $[Fe/H]$ at constant M/L_B. They are listed in Table 4 (columns 2 to 4) for the intermediate galaxy mass M' with $x_1 = 0, 1, 2, 3$. Table 4 shows that the mentioned dispersion in M/L_B ratio (at constant $[Fe/H]$) affects x_3 marginally (by less than 5%), whereas x_2 can be changed by up to 13%. The scatter of $[Fe/H]$ (at constant M/L_B) only produces a change of x_2 (by 8% at most), whereas Δx_3 in practically zero (in agreement with Table 3). Analogously, small changes are brought about by variations of the IMF upper mass: when m_u is changed from 100 to 120 (or 60),x_3 varies by 0.04 (or -0.2) at most, while x_2 is practically unchanged in both cases.

All the results in Sect. s 4.1 and 4.2 are obtained by adopting the fixed value x (or x_2) =2.35 in Eq. (4) to evaluate $[Fe/H]$. Table 2 shows that the maximum differences $(x_2 - 2.35)$ occur for M_1 at $x_1 = 3$ and for M_2 at $x_1 = 0$. The iterative procedure, mentioned at the beginning of Sect. 4, is applied to the latter two cases. At constant M/L_B we obtain in the following order: $[Fe/H] = -0.387$, x_2=1.35, and x_3=3.21 for M_1 with x_1=3; $[Fe/H] = -0.040$, x_2=4.01, and x_3=1.91 for M_2 with x_1=0. These exact solutions, except for $[Fe/H]$, are nearly coincident with the corresponding values listed in Table 2.

4.4. Luminosity-weighted metallicities

According to the assumptions made in Sect. 2.3, the mean metallicities of model ellipticals 15 Gyr old considered so far, are in fact averages by mass. We now compare the observed metallicities based on (4) with the average metallicities of model ellipticals evaluated by weighting abundance Z of each stellar population with luminosity L_V or L_B (taken from B89) in the V and B bands, respectively. We shall adopt the notation $[Fe/H]_B$=log$< Z >_B /Z_\odot$ and $[Fe/H]_V$= log$< Z >_V /Z_\odot$ (whereas $[Fe/H]$ holds its usual meaning of average by mass). As a rule, the exponent x (or x_2) in Eq. (4) is determined iteratively.

Table 5 lists the results for the single-slope IMF and for masses M_1, M', and M_2 (first column) with their reference

Table 5. Single-slope IMF: mass exponent x, lower star mass m_l, and mass averaged $[Fe/H]$ when the observed metallicities according to (4) are approximated by luminosity-weighted model metallicities $[Fe/H]_B$ or $[Fe/H]_V$ (see Sect. 4.4)

M	M/L_B	x	m_l	$[Fe/H]_B$	$[Fe/H]$	x	m_l	$[Fe/H]_V$	$[Fe/H]$
M_1	4.96	2.73	0.223	-0.425	-0.261	2.74	0.220	-0.426	-0.293
M'	8.60	2.49	0.123	-0.180	-0.010	2.51	0.121	-0.181	-0.044
M_2	14.93	2.27	0.040	0.059	0.226	2.28	0.039	0.059	0.192

Table 6. Multi-slope IMF: mass exponents x_2 and x_3 and mass averaged $[Fe/H]$ when observed metallicities according to (4) are approximated by luminosity-weighted model metallicities $[Fe/H]_V$ (see Sect. 4.4)

		$x_1 = 0$	$x_1 = 1$	$x_1 = 2$	$x_1 = 3$
M_1	x_2	2.56	2.23	1.82	1.04
	x_3	2.79	2.89	3.00	3.22
	$[Fe/H]_V$	-0.416	-0.401	-0.394	-0.382
	$[Fe/H]$	-0.287	-0.281	-0.281	-0.284
M'	x_2	3.27	2.98	2.55	2.01
	x_3	2.29	2.37	2.49	2.64
	$[Fe/H]_V$	-0.227	-0.209	-0.184	-0.167
	$[Fe/H]$	-0.065	-0.056	-0.044	-0.040
M_2	x_2	3.79	3.51	3.12	2.58
	x_3	1.88	1.95	2.06	2.20
	$[Fe/H]_V$	-0.027	-0.010	0.013	0.045
	$[Fe/H]$	0.147	0.157	0.171	0.186

M/L_B values (column 2). Columns 3 and 4 give x and m_l, respectively, when $[Fe/H]_B$ (in column 5) is constrained by Eq. (4); the corresponding $[Fe/H]$ is listed in column 6. Analogously, columns 7 to 10 give the solutions when $[Fe/H]_V$ is constrained by Eq. (4). From Table 5 the metallicity $[Fe/H]$ always appears to be larger than the observed metallicities $[Fe/H]_B$ and $[Fe/H]_V$ by 0.165 and 0.133, respectively. Moreover, x and m_l are nearly the same for both $[Fe/H]_B$ and $[Fe/H]_V$, and are only marginally different from those given in Sect. 4.1, as can be inferred from Eq. s (9) and the following relations interpolated in Table 5

$$x = -0.947\ [Fe/H]_V + 2.337 = -0.960\ \log\frac{M}{L_B} + 3.408 \tag{12}$$

$$m_l = -0.371\ [Fe/H]_V + 0.061 = -0.376\ \log\frac{M}{L_B} + 0.481$$

for $2.28 \lesssim x \lesssim 2.74$ and $0.04 \lesssim m_l \lesssim 0.22$. Eq. s (12) give $x = 2.55\ m_l + 2.181$.

The results for multi-slope IMFs are listed in Table 6 for the galaxy masses under study (first column). Quantities x_2, x_3, $[Fe/H]_V$, and $[Fe/H]$ are given for x_1=0, 1, 2, and 3; in each case $[Fe/H]_V$ is bound to satisfy Eq. (4). With regard to solutions for $[Fe/H]_V$, solutions for $[Fe/H]_B$ are as follows: x_2 is smaller by about 0.05, x_3 is practically unchanged, and $[Fe/H]$ is larger by 0.033.

Table 6 shows that $[Fe/H]$ is larger than $[Fe/H]_V$ by about 0.1 to 0.17, depending on x_1 and M according to

$$[Fe/H] \simeq [Fe/H]_V + 0.017\ y - 0.006\ y^2 - 0.007\ x_1 - 0.006\ x_1^2 + 0.162$$

Comparison with Table 2 shows that x_2 is smaller by about 0.1 to 0.2 and x_3 by about 0.01 to 0.03, than the analogous solutions found in Sect. 4.2. The trends of x_2 and x_3 with x_1 and M are essentially preserved, as can be seen from Eq. s (10) and the following relations derived from Table 6

$$x_2 \simeq 0.472\ y - 0.057\ y^2 - 0.227\ x_1 - 0.067\ x_1^2 + 3.273 \tag{13}$$

$$x_3 \simeq -0.351\ y + 0.026\ y^2 + 0.061\ x_1 + 0.020\ x_1^2 + 2.292$$

or, to a first order approximation,

$$x_2 + 3.4\ x_3 \simeq -0.721\ y + 11.067 \tag{14}$$

$$x_2 + 1.35\ x_3 + (0.200\ x_1 + 0.362)^2 \simeq 6.498$$

for $0 \leq x_1 \lesssim 3.5$ and $-1.3 \leq y \leq 1.3$.

5. Discussion and conclusions

The hypothesis worked out in this paper, and concerning M/L_B ratios of elliptical galaxies, contains unavoidable approximations and assumptions dictated by the many free parameters involved. However, they are not unreasonable. For instance, the adopted multi-slope IMF is a generalization of that advocated by Scalo (1986) for the galactic disk, and the simple-model approach follows a suggestion from recent findings (Rich 1990 and 1992; McWilliam & Rich 1994) related to the galactic bulge.

The observational 12% uncertainty in M/L_B would imply,for any given x_1, a fine tuning of x_3 and x_2 (although less stringently) with M/L_B or M, as already found according to other conjectures, as mentioned in Sect. 1 (Renzini & Ciotti 1993; Ciotti et al. 1996). However, this tuning is less evident

when further uncertainties are considered. In Sect. 2.4 we estimate that, as a consequence of the present observational and theoretical deficiences, an (at least) ± 0.2 dex uncertainty in the average $[Fe/H]$ or $[Fe/H]_V$ is to be expected. Moreover, there is an (at least) 20% uncertainty in the computed M/L_B ratio from existing synthetic models (Charlot et al. 1996).

In order to evalute how those uncertainties affect the results, we use Eq. s (9) or (10) for the single-slope IMF. We find that the largest effects are those from $\Delta[Fe/H] = \pm 0.2$ implying $\Delta x = \mp 0.2$ and $\Delta m_l = \mp 0.07$, i.e. nearly half of the full range encompassed by x and m_l. For the multi-slope IMF, x_1 is a free parameter not constrained (as yet) by existing observations and is varied from 0 to 3.5. Tables 2 and 6 show that, for any given M, x_2 and x_3 can be found within a range of about 1.3 and 0.4 width, respectively, i.e. a significant fraction of the full range spanned by x_2 and x_3 when M is increased from M_1 to M_2.

Considering now the multi-slope IMF, it turns out that x_3 always decreases for an increasing M: this behaviour is consistent with the reported non-solar Mg/Fe ratios in ellipticals (Faber et al. 1992; WFG; Weiss et al. 1995). Indeed, adopting Type Ia supernovae (SNeIa) progenitors in the mass range 3 to 8 $M_\odot$ (Greggio & Renzini 1983), and Type II supernovae (SNeII) progenitors in the mass range 8 to 100 $M_\odot$, the number ratio of the SNeII progenitors to the SNeIa progenitors increases for a decreasing x_3. This behaviour is consistent with a Mg/Fe ratio increasing with M, according to the common belief that the SNeII and SNeIa are the major contributors of magnesium and iron, respectively, to the interstellar medium. As far as x_2 is concerned, it turns out from Sect. 4.4 that $\mathrm{d}x_2/\mathrm{d}M \leq 0$ or ≥ 0 according to whether $\mathrm{d}x_3/\mathrm{dlog}M \leq 0.21$ or ≥ 0.21. The different behaviour of x_2 with M entails a different time-evolution of elliptical luminosity with M, according to the relation

$$\frac{\partial M_V}{\partial \mathrm{ln}t} = 1.57 - 0.27\, x_2 \qquad (15)$$

where M_V is the visual absolute magnitude (in the galaxy rest frame) and t is in Gyr (Tinsley & Gunn 1976; Tinsley 1978; Buzzoni 1995).

We can summarize our major results as follows:

i) We explored in some detail the proposal that the observational $M/L_B - M$ relation of elliptical galaxies could be ascribed to a systematic trend of the IMF with galaxy mass M. We adopted a power-law IMF with three slopes ($x_1,\ x_2,\ x_3$) and take into account a $[Fe/H] - M$ relation to further constrain solutions. Results from stellar population synthesis and simple model of chemical evolution were used as basic ingredients.

ii) A single-slope IMF can fit observations at the cost of a practical removal of low-mass stars ($m \lesssim 0.24$), whereas three-slope IMF solutions can be found irrespectively of the predominance of low-mass stars (with $m < 0.3$). Moreover, one has $x_2 + 3.4\, x_3 \simeq -0.72\, \mathrm{log}M + 18.987$, independently of x_1.

Acknowledgements. We thank M. Friedjung for the english revision and the referee H. Krueger for his suggestions which contributed appreciably to improve the paper.

References

Angeletti L., Giannone P., 1990, A&A 234, 53
Angeletti L., Giannone P., 1991, A&A 248, 45
Angeletti L., Giannone P., 1997, in preparation
Arimoto N., Yoshii Y., 1987, A&A 173, 23
Bender R., Burstein D., Faber S.M., 1992, ApJ 399, 462 (BBF)
Bressan A., Chiosi C., Fagotto F., 1994, ApJS 94, 63
Buzzoni A., 1989, ApJS 71, 817 (B89)
Buzzoni A., 1995, ApJS 98,69
Buzzoni A., Gariboldi G., Mantegazza L., 1992, AJ 103, 1814 (BGM)
Carollo C.M., Danziger I.J., Buson L., 1993, MNRAS 265, 553
Charlot S., Worthey G., Bressan A., 1996, ApJ 457, 625
Ciotti L., Lanzoni B., Renzini A., 1996, MNRAS 282, 1
Copeland H., Jensen J.O., Jorgensen H.E., 1970, A&A 5, 12
Davies R.L., Sadler E.M., Peletier R.F., 1993, MNRAS 262, 650 (DSP)
Djorgovski S., Davis M., 1987, ApJ 313, 59
Djorgovski S., Santiago B.X., 1993, Danziger I.J., Zeilinger W.W., Kjar K. (eds.). In: Structure, Dynamics and Chemical Evolution of Elliptical Galaxies, ESO, Garching, p. 59
Dressler A., Lynden-Bell D., Burnstein D., et al., 1987, ApJ 313, 42 (D87)
Faber S.M., Worthey G., Gonzalez J.Jesús, 1992, Barbuy B., Renzini A. (eds.). In: The Stellar Populations of Galaxies, Kluwer, Dordrecht, p. 255
Franx M., Illingworth G.D., 1990, ApJ 359, L41
Freedman W.L., Madore B.F., Mould J.R., et al., 1994, Nat 371, 757
Greggio L., Renzini A., 1983, A&A 118, 217
Guzmán R., Lucey J.R., Bowen R.G., 1993, MNRAS 265, 731
Hills J.G., 1980, ApJ 235, 956
Mathieu R.D., 1983, ApJ 267, L97
McWilliam A., Rich R.M., 1994, ApJ 91,749
Pagel B.E.J. 1989, Beckmann J.E., Pagel B.E.J. (eds.). In: Evolutionary Phenomena in Galaxies, Cambridge University Press, Cambridge, p. 201
Pagel B.E.J., Patchett B.E., 1975, MNRAS 172, 13
Pierce M.J., Welch D.L., Mc Clure R.D., et al., 1994, Nat 371, 385
Renzini A., Buzzoni A., 1986, Chiosi C., Renzini A. (eds.). In: Spectral Evolution of Galaxies, Reidel, Dordrecht, p. 195
Renzini A., Ciotti L., 1993, ApJ 416, L49
Rich R.M., 1990, ApJ 362,604
Rich R.M., 1992, Barbuy B., Renzini A. (eds.). In: The stellar Populations of Galaxies, Kluwer, Dordrecht, p. 29
Scalo J., 1986, Fund. Cosmic Phys. 11, 1
Schaller G., Schaerer D., Meynet G., Maeder A., 1992, A&AS 96, 269.
Tinsley B.M., 1978, ApJ 222, 14
Tinsley B.M., Gunn J.E., 1976, ApJ 203, 52
VandenBerg D.A., Laskarides P.G., 1987, ApJS 64, 103
Weiss A., Peletier R.F., Matteucci F., 1995, A&A 296, 73
Woosley S.E., 1987, Hauck B., Maeder A., Meynet G. (eds.). In: Nucleosynthesis and Chemical Evolution, 16-th Saas Fee Course, Geneva Observatory, Geneva, p. 1
Worthey G., 1994, ApJS 95, 107 (W94)
Worthey G., Faber S.M., Gonzalez J. Jesús, 1992, ApJ 398, 69 (WFG)
Young P.J., 1976, AJ 81,807

This article was processed by the author using Springer-Verlag LaTeX A&A style file *L-AA* version 3.